Journal of Experimental Botany, Vol. 64, No. 5, pp. 1317–1332, 2013
doi:10.1093/jxb/ert015 Advance Access publication 11 February, 2013
This paper is available online free of all access charges (see http://jxb.oxfordjournals.org/open_access.html for further details)

Journal of Experimental Botany
www.jxb.oxfordjournals.org

RESEARCH PAPER

Cessation of photosynthesis in *Lotus japonicus* leaves leads to reprogramming of nodule metabolism

Daniela Tsikou[1], Chrysanthi Kalloniati[1], Mariangela N. Fotelli[1], Dimosthenis Nikolopoulos[1], Panagiotis Katinakis[1], Michael K. Udvardi[2], Heinz Rennenberg[3,4] and Emmanouil Flemetakis[1,*]

[1] Department of Agricultural Biotechnology, Agricultural University of Athens, Iera Odos 75, 11855 Athens, Greece
[2] The Samuel Roberts Noble Foundation, Plant Biology Division, 2510 Sam Noble Pky, Ardmore, OK 7340, USA
[3] Albert-Ludwigs-University Freiburg, Institute of Forest Botany and Tree Physiology, Chair of Tree Physiology, Georges-Köhler-Allee 053/054, D-79110 Freiburg, Germany
[4] King Saud University, PO Box 2454, Riyadh 11451, Saudi Arabia

*To whom correspondence should be addressed. E-mail: mflem@aua.gr

Received 28 September 2012; Revised 3 December 2012; Accepted 17 December 2012

Abstract

Symbiotic nitrogen fixation (SNF) involves global changes in gene expression and metabolite accumulation in both rhizobia and the host plant. In order to study the metabolic changes mediated by leaf–root interaction, photosynthesis was limited in leaves by exposure of plants to darkness, and subsequently gene expression was profiled by real-time reverse transcription–PCR (RT–PCR) and metabolite levels by gas chromatography–mass spectrometry in the nodules of the model legume *Lotus japonicus*. Photosynthetic carbon deficiency caused by prolonged darkness affected many metabolic processes in *L. japonicus* nodules. Most of the metabolic genes analysed were down-regulated during the extended dark period. In addition to that, the levels of most metabolites decreased or remained unaltered, although accumulation of amino acids was observed. Reduced glycolysis and carbon fixation resulted in lower organic acid levels, especially of malate, the primary source of carbon for bacteroid metabolism and SNF. The high amino acid concentrations together with a reduction in total protein concentration indicate possible protein degradation in nodules under these conditions. Interestingly, comparisons between amino acid and protein content in various organs indicated systemic changes in response to prolonged darkness between nodulated and non-nodulated plants, rendering the nodule a source organ for both C and N under these conditions.

Key words: Carbon starvation, *Lotus japonicus*, metabolomic analysis, nodule, symbiosis, transcript profile.

Introduction

Symbiotic nitrogen fixation (SNF) by rhizobia in legumes is a beneficial interaction that provides the plant with the limiting macronutrient nitrogen. SNF takes place in specialized plant organs called nodules. During symbiosis, the plant provides its endosymbiont with photosynthate in exchange for reduced nitrogen, in the form of ammonium and amino acids (Udvardi and Day, 1997; White *et al*., 2007).

SNF creates substantial demand for fixed carbon, rendering the nodule a strong sink for carbohydrates. The carbohydrate supply is derived from plant photosynthates, transported to the nodules via the phloem (Gordon *et al*., 1999). Sucrose is the principal source of carbohydrate and energy for nodule metabolism. Mutants of *Pisum sativum* which lack sucrose synthase activity are not able to produce nitrogen-fixing nodules, indicating that the enzyme is essential for nitrogen fixation (Gordon *et al*., 1999). However, in *Lotus japonicus*, mutants lacking the major nodule-induced isoform of sucrose synthase (*Lj*SUS3) retained some capacity for nitrogen fixation, although they exhibited N stress symptoms (Horst *et al*., 2007). In addition to sucrose synthase, alkaline/neutral

invertase is also important for sucrose degradation, since it releases hexoses. The activity of both enzymes is elevated in *L. japonicus* nodules (Flemetakis *et al*., 2006). The products of sucrose metabolism can be further metabolized by glycolytic enzymes, producing phosphoenolpyryvate (PEP). In *L. japonicus*, >20 genes involved in sugar breakdown have been found to be more highly expressed in nodules than in roots. These highly expressed genes include genes for the majority of the enzymatic steps between sucrose and PEP (Colebatch *et al*., 2004). It is widely accepted that dicarboxylic acids and not sugars are supplied to bacteroids, and transporters that deliver dicarboxylates to the bacteroids have been characterized (Udvardi *et al*., 1988; Jeong *et al*., 2004). PEP can be carboxylated to oxaloacetate and then reduced to malate, the primary source of carbon for bacteroid metabolism and SNF (Day and Copeland, 1991; Streeter, 1995). Both PEP carboxylase (PEPC) and malate dehydrogenase genes have been found to be nodule induced in *L. japonicus* (Colebatch *et al*., 2002; Nakagawa *et al*., 2003; Colebatch *et al*., 2004).

Carbon skeletons generated by carbohydrate breakdown are required to convert ammonium into amino acids. In nodules, ammonium is assimilated into glutamine by the combined activity of the enzymes glutamine synthetase (GS; EC 6.3.1.2) and glutamate synthase (GOGAT; EC 1.4.1.13) (GS/GOGAT pathway) (Patriarca *et al*., 2002; Barsch *et al*., 2006). Asparagine can be produced from the assimilated glutamine via the concerted activity of glutamine-dependent asparagine synthetase (AS; EC 6.3.5.4) and aspartate aminotransferase (ASAT; EC 2.6.1.1). Temperate legumes export asparagine from the nodules to the shoot, but tropical legumes export ureides (Temple *et al*., 1998; Goggin *et al*., 2003). A number of genes involved in ammonium assimilation and asparagine synthesis (including GS and AS) were induced in *L. japonicus* nodules (Colebatch *et al*., 2004).

SNF relies on photosynthate supply (Hardy and Havelka, 1976); consequently, SNF should vary together with photosynthesis. Experimental conditions that enhance photosynthesis, for example an increase in light intensity (Lawn and Brun, 1974; Hardy and Havelka, 1976; Bethlenfalvay and Phillips, 1977), are usually associated with an increase in SNF, whereas experimental conditions that limit photosynthesis, for example shading (Tricot, 1993) and limited light intensity (Feigenbaum and Mengel, 1979), decrease SNF. Extended darkness has been used to study the significance of photosynthetic carbon allocation for nodule metabolism, although a global view of transcriptomic and metabolomic changes in nodules upon carbohydrate limitation is lacking. Responses of nodules to photosynthate limitation vary amongst legume species. For example, the observed decline of nitrogenase activity after prolonged darkness was much less dramatic in soybean (Sarath *et al*., 1986) and cluster bean (Swaraj *et al*., 1994) than it was in common bean (Gogorcena *et al*., 1997) and pea (Matamoros *et al*., 1999). Exposure of nodulated soybeans to a short period of darkness was sufficient to cause a significant decline in the levels of gene transcripts for the key nodule proteins, leghaemoglobin, sucrose synthase, and glutamine synthase, and in the activity of sucrose synthase in nodules (Gordon *et al*., 1993). Furthermore, during dark-induced stress in soybean, a decline in sugars and some key glycolytic intermediates in nodules coincided with depletion of glutamine, asparagine, and alanine, and with accumulation of ureides, which reflected a large reduction of N_2 fixation (Vauclare *et al*., 2010). Moreover, dark exposure decreased respiration and nitrogenase activity of soybean and lupine nodules (Layzell *et al*., 1990; Iannetta *et al*., 1993), indicating that depletion of sucrose in the nodules limits the supply of respiratory substrates to bacteroids and affects SNF. In common bean plants, nitrogenase activity was almost zero after 1 d of darkness and the activities of enzymes involved in carbon and nitrogen metabolism were reduced after 2 d of dark stress (Gorgocena *et al*., 1997).

Previous work on the effect of reduced photosynthesis on nodule metabolism focused on just a few genes, enzymes, and/or metabolites. The aim of this study was to assess the global effects of photosynthetic carbon limitation on metabolism in nodules of the model legume, *L. japonicus*. For this purpose, transcriptomic analysis was carried out, using quantitative real-time PCR, and metabolite profiling, using gas chromatography–mass spectrometry (GC-MS), of nodules subjected to photosynthetic carbon deficiency caused by prolonged darkness. In parallel, in order to study the carbon allocation under these conditions, the systemic effects of prolonged darkness on total amino acid and protein content in different organs of nodulated versus non-nodulated plants were measured. The results indicate that changes in nodule metabolism during photosynthate limitation are controlled largely at the transcriptional level. It is also shown, for the first time, that nodules can become a net source of carbon, as well as of nitrogen, for leaves in the absence of photosynthesis.

Materials and methods

Plant material and growth conditions

Lotus japonicus (Gifu B-129) seeds were kindly provided by Dr Jens Stougaard (University of Aarhus, Denmark). The plants were grown in a controlled environment with a 16 h day/8 h night cycle, a 22 °C day/18 °C night temperature regime, and 70% humidity (Handberg and Stougaard, 1992). Prior to germination, seeds were scarified for 5 min with H_2SO_4 and then sterilized for 20 min in a solution containing 2% NaOCl–0.02% Tween-20. Seeds were pre-germinated at 18 °C in the dark for 72 h and the small plants were grown in Hoagland nutrient solution. For the infection with rhizobia, 72 h seedlings were transferred into pots containing sand, and spot-infected with a 0.1 OD_{600} suspension culture of *Mesorhizobium loti* (strain R7A).

After a 4 week growth period, the plants were divided into groups subjected to the following different light regimes: (i) a normal photoperiod; (ii) a 24 h dark period; (iii) a 24 h dark period followed by 48 h recovery to the normal photoperiod; (iv) a 72 h dark period; and (v) a 72 h dark period followed by 48 h recovery to the normal photoperiod. Nodule harvest was performed between 2 h and 4 h after the beginning of the light period. Nodules of plants exposed to continuous darkness were also harvested at the same time of the day, under green light.

Starch staining

Whole plants of *L. japonicus* were subjected to starch staining. The plants were submerged in boiling water for 1 min and then were transferred to boiling ethanol for the removal of chlorophyll. As soon as the chlorophyll was removed, the plants were rinsed in water and the starch was stained by using a potassium iodide (KI) solution.

For nodule starch staining, nodules were dipped into Jung tissue freezing medium (Leica Microsystems) and cut into thin sections (20 µm) by the use of a Leica CM 1850 cryotome at –15 °C. The sections were transferred onto slides and rinsed in water. The starch was stained by the addition of a few drops of KI solution to the slide. Starch staining visualization was carried out using an Olympus Bx40 microscope equipped with an Olympus DP71 camera.

Nitrogenase activity

Total nitrogenase activity was estimated by the acetylene reduction assay in whole plants at 26 days post-inoculation incubated at 25 °C in 28 ml rubber cap tubes containing 1/10 (v/v) acetylene. The ethylene produced (Supplementary Fig. S2 available at *JXB* online) at different time points (after 1, 2, and 3 h incubation) was quantified with a Perkin-Elmer 8500 gas chromatograph (Perkin-Elmer Life and Analytical Science Inc., Wellesley, MA, USA) equipped with a 2 m Porapak R column and a flame ionization detector. Acetylene reduction activity was calculated from production of ethylene (based on peak area) per mg of nodule dry weight (Hardy *et al*., 1973).

Metabolite extraction, derivatization, and GC-MS analysis

Nodules were harvested, immediately frozen in liquid nitrogen, and lyophilized. Approximately 10 mg dry weight of tissue were ground in liquid nitrogen. Ground samples were extracted with 380 µl of methanol and 20 µl of ribitol in methanol (0.2 mg ml^{-1}). Samples were incubated at 70 °C for 15 min with continuous shaking. After the addition of 200 µl of chloroform, the samples were further incubated at 37 °C for 5 min under continuous shaking. Following the addition of 400 µl of ddH_2O, the samples were vortexed and then centrifuged at 18 000 *g* for 5 min at room temperature. The aqueous phase containing the polar metabolite fraction was transferred into new Eppendorf tubes and dried by nitrogen gas. For derivatization, dried samples were resuspended in 25 µl of methoxyamine-HCl (20 mg ml^{-1} in pyridine), and incubated at 30 °C for 90 min with continuous gentle agitation. This was followed by addition of 50 µl of *N*-methyl-*N*-(trimethylsilyl)-trifluoroacetamide and incubated at 37 °C for 30 min with continuous gentle agitation. Finally, 10 µl of an *n*-alkane mix were added for determination of retention indexes (RIs). Gas chromatography coupled to mass spectrometry (GC-MS) measurements were performed in a Agilent Technologies 7890A GC system coupled to an Agilent Technologies 5975C MS (Agilent Technologies, Frankfurt, Germany). For all treatments tested, five biological replications were conducted. The chromatograms were evaluated automatically using the AMDIS software, and metabolites were identified using the Golm metabolome (Kopka *et al*., 2005; Schauer *et al*., 2005), and Agilent Fienh metabolite and NIST05 metabolite databases. Results are expressed as a response that corresponds to the ratio between the area of the target metabolite divided by the area of the reference metabolite (ribitol, *m/z* 319) and reported relative to the dry weight.

Determination of transcript levels using quantitative real-time reverse transcription–PCR

Lotus japonicus nodules and uninfected roots were harvested and ground in liquid nitrogen. Total RNA was isolated and treated with DNase I (Promega, Madison, WI, USA) at 37 °C for 45 min, in order to eliminate any traces of genomic DNA. Successful removal of genomic DNA was tested by PCR. First-strand cDNA was reverse transcribed from 2 µg of DNase-treated total RNA. All samples were denatured at 65 °C for 5 min followed by quick cooling on ice in a 12 µl reaction mixture containing 500 ng of $oligo(dT)_{12–18mer}$ and 1 µl of 10 mM dNTPs. After the addition of 4 µl of 5× First-Strand buffer (Invitrogen, Paisley, UK), 1 µl (40 U) of RNaseOUT (Invitrogen) RNase inhibitor and 2 µl of 0.1 M dithiothreitol (DTT), the reaction was pre-heated at 42 °C for 2 min before the addition of 1 µl (200 U) of SuperScript II reverse transcriptase (Invitrogen). The reaction mixture was incubated at 42 °C for 50 min, followed by heat inactivation at 70 °C for 15 min. Target cDNAs were amplified using gene-specific primers (Supplementary Table S1 at *JXB* online) designed by the Primer Express 1.5 software (Applied Biosystems, Darmstadt, Germany). Quantitative RT–PCRs were performed on the Stratagene MX3005P using Power SYBR Green master mix (Applied Biosystems), gene-specific primers at a final concentration of 0.2 µM each, and 1 µl of the cDNA as template. PCR cycling started with the initial polymerase activation at 95 °C for 10 min, followed by 40 cycles of 95 °C for 15 s and 60 °C for 1 min. Primer specificity and formation of primer dimers were monitored by dissociation curve analysis. The expression levels of an *L. japonicus* ubiquitin gene were used as internal standards to normalize small differences in cDNA template amounts. Relative transcript levels of the gene of interest (X) were calculated as a ratio to the ubiquitin gene transcripts (U), as $(1+E)^{-\Delta Ct}$, where ΔC_t was calculated as $(C_t^X – C_t^U)$. PCR efficiency (E) for each amplicon was calculated employing the linear regression method on the Log (Fluorescence) per cycle number data, using the LinRegPCR software (Ramakers *et al*., 2003). All real-time qPCRs were performed on three biological repeats.

^{13}C labelling

The ^{13}C labelling was conducted through the root system of 30-day-old inoculated *L. japonicus* plants, as previously described (Fotelli *et al*., 2011). In total, 108 plants were used for the labelling experiment, subjected to the previously described normal photoperiod and extended dark conditions. All plants were placed in vials (100 ml volume) for hydroponics which were connected to a CO_2-free air supply system, during a 2 h acclimation period. CO_2 was removed from the air supply with soda lime CO_2 traps. For dark treatment, the hypergeous part of the plants was covered. Two-thirds of the plants were transferred from hydroponics to air-tight glass vials containing 10 mM $Na_2{}^{13}CO_3$ solutions (99% enriched in ^{13}C; pH=6). $Na_2{}^{13}CO_3$ dissociates in water and produces $^{13}CO_2$ that is taken up by the plants. Labelling was performed by a 2 h pulse. After labelling, one-third of the plants were kept in hydroponics for a 1 h chase period. Nodules were harvested after each phase (2 h acclimation period, 2 h labelling, and 1 h chase period), ground in liquid nitrogen, and stored at –80 °C.

$\delta^{13}C$ composition

Nodules were oven-dried (3 d, 65 °C) and samples of 0.5 mg were transferred into tin capsules (IVA Analysentechnik, Meerbusch, Germany). Subsequently, the samples were injected into an isotope ratio mass spectrometer (Delta Plus; Finnigan MAT GmbH, Bremen, Germany) for $\delta^{13}C$ analysis. $\delta^{13}C$ values are expressed relative to the VPDB (Vienna Pee Dee Belemnite) standard.

Soluble protein

To quantify total soluble protein concentrations, ~0.05 g of frozen tissue were extracted in 1 ml of buffer (0.1 M K_2HPO_4/KH_2PO_4 pH 7.7, 5 mM Na-EDTA, 10 mM DTT, 1% Triton X-100, 2% PVP). The protein extracts were passed through cotton gauze. For quantification of soluble protein, 1 ml of Bradford reagent plus 90 µl of 0.15 M NaCl were added to 10 µl aliquots of the extracts. The optical density was measured in a Hitachi U-2800 Spectrophotometer (Tokyo, Japan) at 595 nm after a 20 min incubation at room temperature in the dark (Bradford, 1976). Bovine serum albumin was used as a standard.

Total amino acid content

For quantification of total soluble amino acids, aliquots of 0.05 g fresh weight of tissue were homogenized in 1 ml of methanol:chloroform (3.5:1.5, v:v) and 0.2 ml of buffer (pH 7.0) containing 20 mM HEPES, 5 mM EGTA, and 10 mM NaF, according to the method of Winter *et al*. (1992). After incubating for 30 min, 600 µl of distilled water were added to the samples, mixed, and centrifuged for 5 min at 14 000 *g* and 4 °C. This step was repeated once. Total amino acid

content was determined from the combined supernatants according to the method of Liu *et al*. (2005). Aliquots of the extract (100 µl) and 100 µl of ninhydrin reagent [50/50 mixture of solution one containing 19.21 g of citrate in 200 ml of 1 N NaOH (pH 5.0), made up to 500 ml with distilled water and 0.8 g $SnCl_2 \cdot H_2O$, and solution two containing 20 g of ninhydrin in 500 ml of ethylene glycol monomethyl ether] were prepared. Isopropanol (800 µl, 50%) was added to the samples, followed by a 15 min incubation at 100 °C. The optical density was measured in a Hitachi U-2800 Spectrophotometer (Tokyo, Japan) at 570 nm. Glutamine was used as a standard.

Statistical analysis

Transcriptomic and metabolomic data statistical analysis was performed by one-way analysis of variance (ANOVA) at a 95% level of significance. Principal components analysis (PCA) was performed using the Unscrambler 9.5 software (CAMO Software Inc., NJ, USA). Missing values were defined as 0, assuming that missing values were unchanged when compared with the co-analysed standard samples. Statistical analysis of data of nodule $\delta^{13}C$ abundance was carried out using SPSS 12.0 (SPSS Inc., Chicago, IL, USA). Comparisons were performed by independent-sample *t*-tests at a 95% level of significance. To detect differences in total protein and total amino acid content between the examined tissues, independent-sample *t*-tests were used at a 95% level of significance. Statistical tests were conducted using Sigmaplot 10.0 statistical software (Systat Software Inc.. San Jose, CA, USA).

Results

Extended dark reduces starch levels and nitrogenase activity

To identify global changes in nodule metabolism under carbohydrate limitation, *L. japonicus* plants were subjected to prolonged darkness. The length of the dark period applied to the plants was determined based on the rate of starch breakdown in nodules. For this reason, starch accumulation was visualized by direct staining in nodules after 12, 24, 36, 60, and 72 h of continuous darkness. After 24 h of continuous darkness, starch deposits were still evident in nodule sections via staining, but after 72 h of darkness starch reserves were completely exhausted (Supplementary Fig. S1 at *JXB* online). Thus, these two time points were selected for further analysis.

The effect of photosynthetic carbon limitation on nitrogenase activity in intact *L. japonicus* nodules was estimated by the acetylene reduction assay, using whole plants. After 24 h of continuous darkness, nitrogenase activity was almost 7-fold reduced compared with control plants exposed to normal photoperiod conditions, while after 72 h of darkness nitrogenase activity was >30-fold reduced compared with the control (Fig. 1). To test whether the reduced nitrogenase activity observed was a direct effect of carbohydrate limitation caused by prolonged darkness, nitrogenase activity was measured after 48 h recovery by transferring the darkened plants back to the normal photoperiod conditions. Nitrogenase activity partially recovered, to almost 60% of its original level, following restoration of the normal photoperiod (Fig. 1).

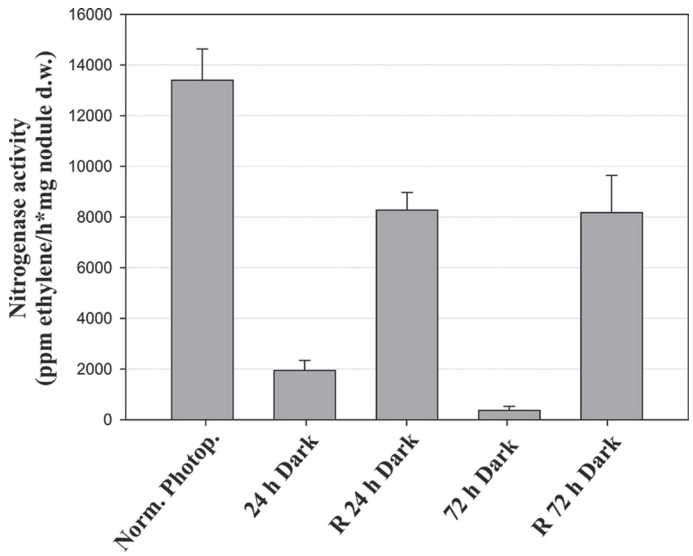

Fig. 1. Nitrogenase activity, assayed as acetylene reduction, in *L. japonicus* nodules under a normal photoperiod, after the plants have been subjected to extended dark periods for 24 h and 72 h, and after 48 h recovery (R) under the normal photoperiod, respectively. Bars represent means (±SE) of six biological replications.

Nodule metabolite profiling under carbon-limiting conditions

For this experiment, 30-day-old nodulated *L. japonicus* plants were subjected to either 24 h or 72 h of continuous darkness, while control plants of the same age were kept under normal photoperiod conditions. GC-MS analysis in nodules identified metabolites belonging to different classes, including amino acids, organic acids, other nitrogenous compounds, sugars, and polyols.

Changes in specific metabolites were calculated by the response ratios for dark-treated versus control plants exposed to normal photoperiod conditions. Although the levels of many metabolites were not significantly different following extended darkness, ANOVA detected 39 metabolites that changed significantly ($P < 0.05$, Table 1). Moreover, seven metabolites were found only in dark-treated plants.

Sucrose levels declined substantially during extended darkness, with a 60% reduction after 72 h of darkness. Raffinose, D-melezitose, maltotriose, and D-glucose concentrations also decreased significantly with prolonged darkness (Table 1). In the organic acid group, significantly reduced concentrations of L-ascorbic acid, succinic acid, pyruvic acid, gluconic acid, glycolic acid, D-malic acid, and oxalic acid were found in nodules of dark-treated plants. Reduced concentrations of phosphates were also measured. *O*-Phospho-L-threonine, pyrophosphate, adenosine-*S*-monophosphate, and D-glucose-6-phosphate were significantly reduced in nodules of dark-treated plants; however, *O*-phosphocolamine accumulation was remarkably high (almost 20-fold). Putrescine, methyl-β-D-galactopyranoside, *N*-methyl-DL-glutamic acid, and 1-methyl-nicotinamide levels also declined significantly following extended darkness.

Table 1. Identified metabolites of L. japonicus nodules harvested from plants grown under normal photoperiod (N. Ph.), or subjected to 24 h and 72 h continuous darkness.

	m\z	RI	PC1 (49%) loadings	PC2 (27%) loadings	N. Ph. average response	24 h darkness average response	72 h darkness average response	24 h/N. Ph. response ratio	72 h/N. Ph. response ratio	*P*-value
Sugars										
Sucrose	361	2385	–0.5010	0.3580	8.679	7.866	3.276	0.91 a	**0.38** b	<0.001
Raffinose	87	3056	–0.0197	–0.0103	0.268	0.060	0.026	**0.22**	**0.10**	0.010
Maltose	361	2495	0.0005	–0.0023	0.059	0.051	0.068	0.86	1.14	0.833
Trehalose	361	2505	0.0144	–0.0178	0.329	0.413	0.492	1.25	1.49	0.310
D-Melezitose	361	3153	–0.0380	–0.0010	0.558	0.231	0.069	**0.41** a	**0.12** b	<0.001
Melibiose	361	2512	–0.0046	0.0043	0.216	0.146	0.155	0.67	0.72	0.208
Cellobiose	361	2252	–0.0002	–0.0006	0.020	0.016	0.015	0.79	0.77	0.870
Maltotriose	361	3034	–0.0031	0.0008	0.039	0.015	0.002	**0.40**	**0.06**	0.012
D-Lyxose	217	1389	–0.0012	0.0001	0.024	0.019	0.011	0.80	0.48	0.393
D-Glucose	319	1614	–0.0187	0.0033	0.237	0.088	0.000	**0.37** a	**0.00** b	0.047
Amino acids										
L-Cysteine	220	1250	0.0047	–0.0030	0.000	0.042	0.047	**Dark sp.**	**Dark sp.**	0.529
L-Ornithine	142	1310	0.0150	–0.0091	0.000	0.000	0.185	ND	**Dark sp.**	–
L-Homoserine	218	1145	0.0103	0.0018	0.017	0.062	0.129	**3.70**	**7.74**	0.028
L-Proline	142	983	–0.0048	0.0025	0.106	0.074	0.042	0.69	0.40	0.603
L-Asparagine	231	1376	0.4410	0.1160	11.782	14.955	17.094	**1.27 a**	**1.45** b	<0.001
β-Alanine	248	1116	0.0057	–0.0005	0.052	0.060	0.119	1.16 a	**2.30** b	0.009
L-Glutamic acid	246	1319	0.1840	0.8760	2.066	5.274	4.310	1.28	1.15	0.211
β-Cyano-L-alanine	141	1064	0.0022	0.0020	0.190	0.201	0.187	1.06	0.98	0.959
L-Alanine	116	798	–0.0252	0.0160	0.400	0.397	0.119	0.99 a	**0.30** b	0.004
L-Serine	204	1055	0.0262	–0.0019	0.330	0.430	0.673	1.31 a	**2.04** b	0.018
L-Aspartic acid	232	1216	0.3470	–0.0640	0.873	2.162	4.931	**2.48** a	**5.65** b	<0.001
L-Lysine	317	1618	0.0722	–0.0294	0.212	0.334	1.066	1.57 a	**5.02** b	<0.001
L-Tyrosine	218	1635	0.0674	0.0217	0.000	0.682	0.778	**Dark sp.**	**Dark sp.**	0.059
L-Methionine	176	1208	0.0066	–0.0036	0.000	0.000	0.070	ND.	**Dark sp.**	–
L-Histidine	154	1618	0.1240	–0.0340	0.065	0.186	1.450	2.88 a	**22.45** b	<0.001
L-Valine	144	903	0.0888	–0.0378	0.106	0.280	1.185	2.65 a	**11.21** b	<0.001
L-Threonine	218	1083	0.0211	–0.0002	0.166	0.343	0.434	**2.07**	**2.62**	<0.001
L-Tryptophan	202	1918	0.0878	–0.0262	0.046	0.350	1.120	**7.64** a	**24.41** b	<0.001
DL-Isoleucine	158	982	0.0768	0.0058	0.034	0.297	0.875	**8.70** a	**25.58** b	<0.001
L-Glutamine	156	1470	–0.0184	–0.0036	0.411	0.129	0.130	**0.31**	**0.32**	<0.001
Glycine	174	993	0.0103	0.0021	0.027	0.097	0.146	**3.55**	**5.35**	0.028
Organic acids										
Dehydroascorbic acid	173	1553	–0.0025	–0.0019	0.036	0.000	0.000	**0.00**	**0.00**	–
Shikimic acid	204	1517	–0.0019	0.0003	0.032	0.000	0.000	**0.00**	**0.00**	–
6-Hydroxycaproic acid	147	1010	0.0017	–0.0011	0.018	0.031	0.033	1.68	1.81	0.626
L-Ascorbic acid	332	1659	–0.0107	–0.0086	0.173	0.041	0.000	**0.24**	**0.00**	0.039
L-Lactic acid	147	765	–0.0097	–0.0093	0.301	0.306	0.206	1.02	0.69	0.519
Succinic acid	148	999	–0.0241	0.0232	0.541	0.677	0.250	1.25 a	**0.46** b	0.006
Pyruvic acid	174	756	–0.0010	–0.0000	0.020	0.012	0.005	**0.61** a	**0.27** b	<0.001
Glyceric acid	189	1024	0.0025	0.0005	0.036	0.038	0.067	1.05	1.87	0.165
Pipecolic acid	156	1051	0.0139	0.0068	0.144	0.171	0.275	1.18	1.90	0.263
Mucic acid	333	1763	0.0003	0.0009	0.317	0.348	0.317	1.10	1.00	0.387
Citric acid	347	1529	–0.1140	0.0781	8.026	7.309	6.357	0.91	0.79	0.069
Isocitric acid	273	1531	0.0023	0.0029	0.000	0.079	0.056	**Dark sp.**	**Dark sp.**	0.537
Citramalic acid	147	1169	0.1520	0.1640	5.783	8.406	7.776	**1.45**	**1.34**	0.005
Maleic acid	147	989	–0.0018	–0.0019	0.048	0.055	0.025	1.15	0.52	0.502
Fumaric acid	245	1033	–0.0020	0.0002	0.159	0.150	0.119	0.94	0.75	0.187
Glucaric acid	333	1732	–0.0017	0.0010	0.480	0.439	0.434	0.92	0.90	0.843
Gluconic acid	333	1698	–0.0079	0.0038	0.459	0.213	0.255	**0.46**	**0.56**	0.034
2-Hydroxycinnamic acid	293	1397	0.0112	–0.0026	0.668	0.884	0.777	1.32	1.16	0.298

Table 1. Continued

	m\z	RI	PC1 (49%) loadings	PC2 (27%) loadings	N. Ph. average response	24 h darkness average response	72 h darkness average response	24 h/N. Ph. response ratio	72 h/N. Ph. response ratio	*P*-value
4-Hydroxycinnamic acid	293	1624	–0.0011	–0.0023	0.038	0.042	0.015	1.09	0.40	0.464
Citraconic acid	147	1040	–0.0000	0.0001	0.002	0.004	0.001	2.32	0.77	0.437
Glycolic acid	147	775	–0.0008	0.0002	0.023	0.012	0.008	**0.53**	**0.35**	0.021
Malonic acid	147	890	–0.0094	0.0005	0.736	0.732	0.671	1.00	0.91	0.926
D-Malic acid	147	1187	–0.3360	0.1160	5.901	5.240	1.798	0.89 a	**0.30** b	<0.001
Oxalic acid	147	824	–0.0130	0.0027	0.325	0.272	0.177	0.84 a	**0.54** b	0.013
Polyols										
Galactinol	204	2708	–0.0070	–0.0037	0.092	0.031	0.010	0.33	0.11	0.101
Palatinitol	361	2555	0.0011	0.0009	0.034	0.036	0.053	1.06	1.56	0.417
D-Mannitol	319	1648	0.0471	0.1800	0.477	1.643	1.161	**3.45**	2.43	0.020
Pinitol	260	1550	–0.4390	–0.0313	22.215	22.108	18.608	1.00	0.84	0.223
allo-Inositol	318	1745	–0.0008	–0.0010	0.216	0.202	0.201	0.94	0.93	0.984
Phosphates										
O-Phospho-L-threonine	370	1534	–0.0026	–0.0008	0.037	0.000	0.000	**0.00**	**0.00**	–
Phosphoric acid	299	967	–0.0072	0.0056	3.422	2.796	3.168	0.82	0.93	0.245
Phosphoenolpyruvic acid	369	1302	0.0014	–0.0000	0.008	0.012	0.028	1.57 a	**3.68** b	0.007
O-Phosphocolamine	299	1485	0.0161	–0.0036	0.010	0.089	0.203	**8.79** a	**19.97** b	<0.001
Pyrophosphate	451	1377	–0.0013	0.0001	0.021	0.009	0.003	**0.41**	**0.16**	<0.001
Adenosine-5-monophosphate	315	2751	–0.0188	–0.0008	0.366	0.161	0.111	**0.44** a	**0.30** b	<0.001
3-Phosphoglycerate	357	1519	0.0015	–0.0044	0.116	0.018	0.134	0.16	1.16	0.291
3-Phosphoglyceric acid	387	1519	0.0028	0.0034	0.086	0.096	0.132	1.12	1.53	0.232
D-Glucose-6-phosphate	387	2052	–0.0221	–0.0051	0.348	0.144	0.098	**0.41**	**0.28**	0.019
Uridine 5'-monophosphate	315	2563	–0.0029	–0.0003	0.044	0.074	0.030	1.65	0.69	0.181
Glycerol 1-phosphate	357	1471	–0.0011	–0.0011	0.155	0.151	0.126	0.97	0.82	0.556
Other metabolites										
Putrescine	174	1427	–0.0014	–0.0003	0.063	0.045	0.037	**0.73**	**0.59**	0.009
Spermidine	174	1952	–0.0010	–0.0004	0.043	0.043	0.024	1.01	0.56	0.320
Uracil	241	1021	0.0001	–0.0004	0.021	0.009	0.015	0.45	0.73	0.619
Urea	147	922	0.0009	–0.0023	0.013	0.034	0.035	2.63	2.75	0.488
Adenine	264	1555	–0.0014	0.0010	0.019	0.025	0.013	1.32	0.65	0.440
Adenosine	236	2342	0.0004	0.0066	0.028	0.111	0.053	**3.96** a	1.88 b	0.007
Norvaline	72	783	0.0004	0.0008	0.000	0.006	0.007	**Dark sp.**	**Dark sp.**	0.246
Loganin	361	2539	0.0032	0.0032	0.254	0.290	0.287	1.14	1.13	0.557
Thymine	255	1057	0.0003	0.0004	0.011	0.024	0.015	2.14	1.35	0.235
L-Norleucine	158	960	0.0206	0.0045	0.014	0.163	0.226	**11.39**	**15.79**	0.040
Porphine	285	1020	0.0013	0.0012	0.008	0.024	0.028	2.91	3.38	0.146
Trans-3-hydroxy-L-proline	230	1221	0.0002	–0.0001	0.000	0.001	0.002	**Dark sp.**	**Dark sp.**	0.186
Methyl-β-D-galactopyranoside	204	1699	–0.0177	–0.0082	0.482	0.258	0.229	**0.54**	**0.48**	<0.001
N-methyl-D-glutamic acid	260	1382	–0.0086	–0.0006	0.110	0.197	0.033	1.78 a	**0.30** b	0.009
1-Methyl-nicotinamide	179	1155	–0.0009	–0.0004	0.015	0.005	0.002	0.31	**0.11**	0.011

For each identified metabolite, GC-MS characteristics (fragment mass, RI, retention index), loadings in principal components of Fig. 3, average response (resulting from five biological replications), and response ratios of each dark period to the normal photoperiod are presented.

Response ratios representing significant differences ($P < 0.05$) are indicated in bold, while significant differences between the relative responses measured after 24 h and 72 h darkness are indicated by different letters. The *P*-value represents the level of significance between the relative responses of each compound (ANOVA), when at least two average responses are >0.

In most metabolite groups, significantly dark-affected compounds declined under darkness, with the highest reductions being observed after 72 h of continuous darkness. PCA, which allows clustering of samples into groups, revealed strong differentiation in metabolite contents after 72 h of continuous darkness. The first PCA component accounted for 49% of the variance in metabolite levels and separated samples of 72 h darkness from those of 24 h darkness and the normal photoperiod. According to the first component, 24 h of darkness exhibited similarity to the normal photoperiod; however, the second component, which accounted for 27% of the variance, allowed distinction between samples of 24 h darkness and the normal photoperiod (Fig. 2A).

A remarkable exception to the trend of reduced metabolite levels following prolonged darkness was the high accumulation of certain amino acids. In this compound group, most of the identified metabolites were found at significantly higher concentrations under continuous darkness. These included DL-isoleucine, L-tryptophan, and L-histidine, which exhibited 25-, 24-, and 22-fold increased levels after 72 h of darkness, respectively. Nine other amino acids were also found to accumulate under these conditions, with L-valine and L-homoserine presenting the highest accumulation. In addition, four amino acids (L-cysteine, L-ornithine, L-tyrosine, and L-methionine) were detected exclusively in nodules of dark-treated plants (Table 1). In PCA analysis, the first component was influenced most by three amino acids: L-asparagine, L-aspartic acid, and L-glutamic acid (Fig. 2B), which is indicative of the strong differentiation of amino acids under these conditions.

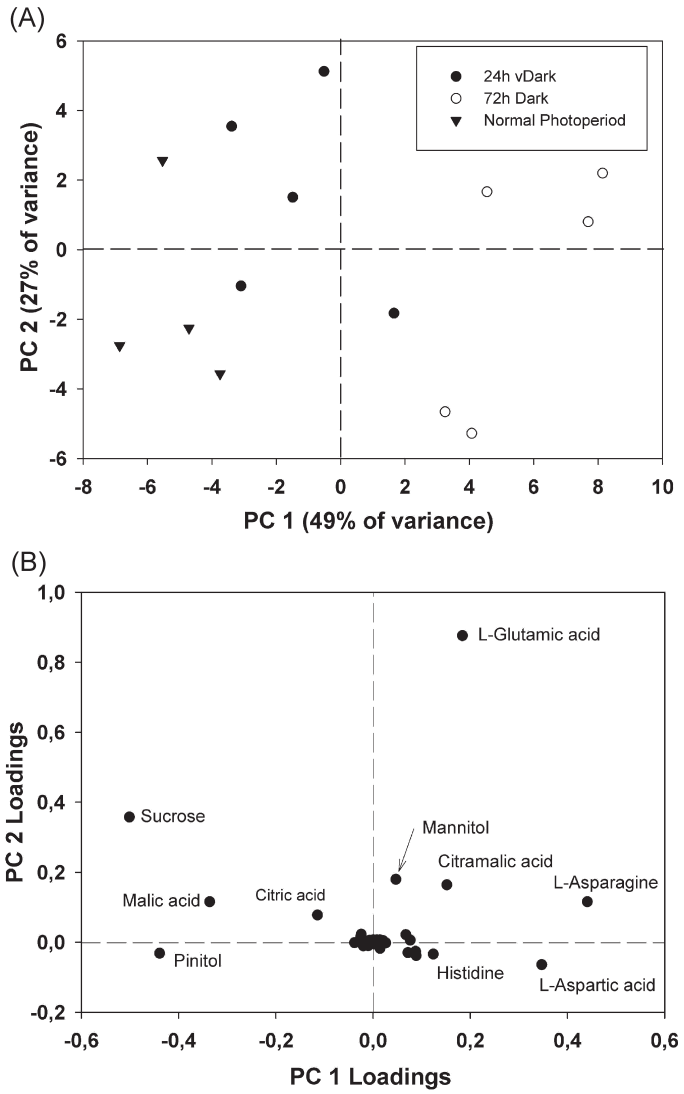

Fig. 2. Principal component analysis of GC-MS profiles of *L. japonicus* nodules harvested from plants grown under a normal photoperiod (n=4), and after the plants have been subjected to 24 h and 72 h of a continuous dark period (n=5). (A) Bi-plot of principal components 1 and 2 representing 76% of the total variance observed in the GC-MS profiles. (B) Loadings of individual indentified components showing the highest variability under the studied experimental conditions.

Transcriptional regulation of plant genes in nodules under carbon-limiting conditions

Gene transcript profiling was studied in nodules of plants exposed to the normal photoperiod, and extended dark for 24 h and 72 h. Gene transcripts were analysed by quantitative real-time PCR (qRT-PCR) using a platform containing 174 gene-specific primer pairs (Supplementary Table S1 at *JXB* online) for genes involved in various aspects of nodule metabolism (Ott *et al*., 2009). Most genes represented on the qRT-PCR platform code for enzymes involved in primary metabolic processes in nodules such as starch metabolism, carbohydrate metabolism, pentose phosphate cycle, tricarboxylic acid (TCA) cycle, glycolysis, CO_2 fixation, ammonium assimilation, and amino acid metabolism.

To identify changes in gene expression under photosynthetic carbon-limiting conditions, transcript levels were measured after 24 h and 72 h of continuous darkness and compared with transcript levels under normal photoperiod conditions. Although transcript levels of many genes represented on the qRT-PCR platform were not significantly different after the extended dark period compared with the control, ANOVA revealed 54 genes that were significantly up- or down-regulated after 24 h of darkness. After 72 h of extended darkness, a total of 89 genes showed significant differences in expression ($P < 0.05$) (Supplementary Table S2 at *JXB* online). The majority of the genes analysed exhibited reduced transcript levels under prolonged darkness, while only a few genes were found to be up-regulated (Fig. 3A).

PCA analysis revealed great differentiation in gene expression after 24 h and 72 h of continuous darkness when compared with gene expression under the normal photoperiod. The first component accounted for 71% of the variance and allowed distinction of the normal photoperiod from extended darkness. According to the first component, 24 h of darkness exhibited similarity to 72 h of darkness; however, the second component, which accounted for 13% of the variance, allowed distinction of 24 h and 72 h of darkness (Fig. 3B).

Many gene transcripts were found to be >5-fold down-regulated in nodules after an extended dark period of 72 h

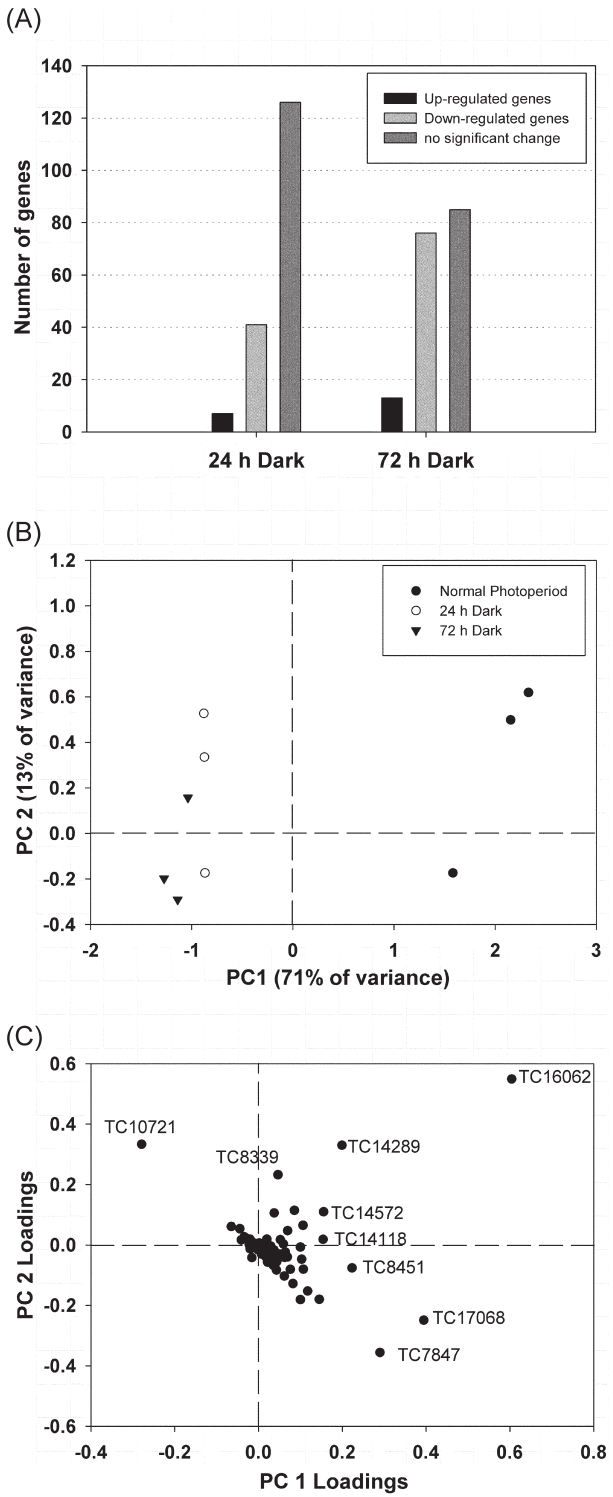

Fig. 3. Analysis of the gene expression profiling results of *L. japonicus* nodules harvested from plants grown under a normal photoperiod, and after the plants have been subjected to 24 h and 72 h of a continuous dark period (n=3). (A) Number of genes showing increased expression levels (ratio dark/normal photoperiod >2, $P < 0.05$), decreased expression levels (ratio dark/normal photoperiod <0.5, $P < 0.05$), or unaffected expression levels ($P > 0.05$). (B) Bi-plot of principal components 1 and 2 representing 84% of the total variance observed in gene expression levels. (C) Loadings of individual gene transcripts showing the highest variability under the studied experimental conditions.

(dark/normal photoperiod ratio <0.2, P <0.05, Table 2). The majority of these genes are involved in starch and sugar metabolism, including two genes encoding ADP-glucose pyrophosphorylases, two genes encoding phosphoglucomutases, and one gene encoding sucrose synthase, which presented a 12.5-fold reduction in expression levels (Table 2). The great differentiation in the expression levels of this gene (TC7847) under extended darkness was also seen by the PCA analysis because it was among the genes that most influenced the first component (Fig. 3C). The expression of genes encoding glycolytic enzymes was also highly reduced after 72 h of darkness. These included genes for two enolases and a pyruvate decarboxylase.

Regarding CO_2 fixation, six genes were found to be >5-fold down-regulated, including three genes encoding carbonic anhydrases and one gene encoding phosphoenolpyruvate carboxylase, which together fix CO_2 into oxaloacetate. Moreover, a 6.5-fold reduction in expression levels was observed in one gene encoding malate dehydrogenase, which uses oxaloacetate as a substrate to produce malate, the main carbon source for bacteroid metabolism and nitrogen fixation.

In the ammonium assimilation metabolic pathway, two genes encoding glutamine synthetase and glutamate dehydrogenase presented a remarkable reduction in their expression levels after both 24 h and 72 h of continuous darkness (Table 2). However, one gene encoding an NADH glutamate dehydrogenase and one gene encoding an asparagine synthase were almost 40- and 20-fold up-regulated, respectively, after 72 h of darkness (Table 3).

Several genes involved in amino acid metabolism were down-regulated after prolonged darkness. Thirteen genes exhibited >5-fold reduction in expression levels, while eight of these had transcript levels that were >10-fold lower than in the control. These included a gene encoding serine acetyltransferase and two genes encoding cysteine synthase, which are involved in cysteine biosynthesis, two genes encoding aspartokinase-homoserine dehydrogenase and threonine synthase, which are involved in threonine biosynthesis, and one gene encoding ornithine cyclodeaminase and two genes encoding prolyl 4-hydroxylase, which are involved in proline metabolism (Table 2). However, in proline metabolism, a remarkable increase was detected in the expression levels of a gene encoding an ornithine aminotransferase and another gene encoding a proline dehydrogenase (Table 3). Significant reduction was observed in the expression levels of many genes involved in flavonoid biosynthesis, lignin biosynthesis, and other aspects of secondary metabolism, including genes encoding chalcone reductase, flavanone 3-hydroxylase, isoliquiritigenin 2'-*O*-methyltransferase, laccase, 4-coumarate, and cytochrome P450 (Table 2). However, there are a number of gene transcripts involved in secondary metabolism which were found to be highly up-regulated (Table 3). The fact that some genes encoding enzymes involved in flavonoid biosynthesis have been detected to be up-regulated and some others down-regulated raises questions about the flavonoid changes in nodules under such conditions.

Table 2. Genes highly down-regulated in nodules after extended dark periods.

Gene	Lotus gene ID	Expression ratio versus control		*P*-value
		24 h/N. Ph.	72 h/N. Ph.	
Starch metabolism				
Soluble starch synthase {*Arabidopsis thaliana*}	TC15963	0.34	**0.17**	0.024
ADP-glucose pyrophosphorylase small subunit PvAGPS1	TC8396 5 end	0.08	**0.02**	0.004
ADP-glucose pyrophosphorylase small subunit CagpS1	TC8756 3 end	0.06	**0.03**	0.011
Other carbohydrate metabolism				
Trehalose-6-phosphate synthase homologue	TC14996	0.12	**0.03**	0.004
Phosphoglucomutase, cytoplasmic	TC14676	0.14	**0.09**	0.025
Phosphoglucomutase, cytoplasmic	TC14675	0.40	**0.07**	0.036
Glucose-6-phosphate isomerase	TC17137	**0.28**	**0.20**	0.033
Sucrose synthase 1	TC7847	0.16	**0.08**	0.004
Glycolysis				
Enolase	TC14118	**0.36**	**0.13**	0.004
Enolase	TC16760	0.73	**0.17**	0.004
Pyruvate decarboxylase II	TC7922	**0.27**	**0.17**	<0.001
Pentose phosphate pathway				
Glucose-6-phosphate 1-dehydrogenase	TC8851	0.29	**0.06**	0.004
Transaldolase	TC11589	0.02	**0.01**	0.011
Transaldolase ToTAL2	TC10369	0.18	**0.08**	0.011
TCA cycle				
Cytosolic malate dehydrogenase (1.1.1.37)	TC7834	0.28	**0.15**	0.011
Aconitate hydratase, cytoplasmic	TC14371	0.37	**0.16**	0.004
CO_2 metabolism				
Carbonic anhydrase LjCA1	TC14306	0.01	**0.00**	0.004
CA α-type	Ljnest13e5	**0.33**	**0.13**	<0.001
CA α-type 2	Ljnest20a7rc	0.20	**0.08**	0.004
Phosphoenolpyruvate carboxylase	TC7830	0.60	**0.11**	0.009
Phosphoenolpyruvate carboxylase kinase	TC14602	0.19	**0.07**	0.004
Ribulose bisphosphate carboxylase/oxygenase activase	TC14081	**0.17**	**0.03**	0.012
Ammonium assimilation				
Glutamine synthetase, cytosolic isozyme	TC8035	**0.39**	**0.13**	0.007
Glutamate dehydrogenase	TC10844	**0.20**	**0.16**	0.008
Other aminoacid metabolism				
Alanine:glyoxylate aminotransferase 2 homologUE	TC9107	0.48	**0.10**	0.016
Histidinol dehydrogenase	TC10151	0.17	**0.06**	0.004
Serine acetyltransferase	TC17048	0.19	**0.05**	0.004
Cysteine synthase	TC14692	0.15	**0.08**	0.011
Plastidic cysteine synthase 1	TC17110	**0.03**	**0.07**	<0.001
Threonine dehydratase/deaminase	TC18952	**0.20**	**0.17**	<0.001
Aspartokinase-homoserine dehydrogenase (HDH)	TC9572	0.07	**0.01**	0.004
Threonine synthase	TC9527	0.20	**0.07**	0.004
Pantoate-beta-alanine ligase	TC12836	**0.19**	**0.14**	<0.001
Similarity to ornithine cyclodeaminase	TC11292	**0.23**	**0.08**	0.001
Prolyl 4-hydroxylase	TC15896	**0.29**	**0.11**	<0.001
Prolyl 4-hydroxylase, alpha subunit-like protein	TC11925	**0.32**	**0.20**	0.005
Branched-chain amino acid aminotransferase-like protein	TC16062	0.13	**0.01**	0.004
Other metabolism				
Chalcone reductase	TC8351	0.01	**0.00**	0.011
Putative flavanone 3-hydroxylase	TC7931	0.40	**0.14**	0.004
Acidic endochitinase	TC14167	**0.16**	**0.04**	<0.001
Thiazole biosynthetic enzyme precursor	TC14068	0.06	**0.02**	0.004
Cytochrome P450	TC15466	**0.33**	**0.04**	0.004
Cytochrome P450	TC8343	**0.05**	**0.01**	<0.001
N-Hydroxycinnamoyl/benzoyltransferase-like protein	TC8570	0.23	**0.08**	0.004
Isoliquiritigenin 2'-O-methyltransferase	TC14525	0.35	**0.17**	<0.001
4-Coumarate:CoA ligase 2	TC7977	0.47	**0.16**	0.003
Laccase	TC17617	0.04	**0.02**	0.025
Pyrroline-5-carboxylate reductase	TC15604	**0.25**	**0.17**	<0.001

Gene expression in *L. japonicus* nodules harvested from plants grown under normal photoperiod (N. Ph.), or subjected to 24 h and 72 h continuous darkness, respectively. Transcript levels of these genes decreased significantly (<5-fold, $P < 0.05$) under extended dark conditions and are marked in bold. The numbers indicate ratios of gene expression after 24 h and 72 h continuous darkness versus expression in the normal photoperiod (control). The *P*-value represents the level of significance between the relative gene expression levels (ANOVA).

Table 3. Genes highly induced in nodules after extended dark periods.

Gene	Lotus gene ID	Expression ratio versus control		*P*-value
		24 h/N. Ph.	72 h/N. Ph.	
Other carbohydrate metabolism				
Trehalase 1	TC18454	1.88	**2.97**	0.007
Beta-fructofuranosidase	TC16805	1.76	**3.56**	0.039
Pentose phosphate pathway				
Ribulose-phosphate 3-epimerase, chloroplast precursor	TC7925	**3.27**	**2.09**	0.004
TCA cycle				
Aconitase (aconitate hydratase) (citrate hydrolyase)	TC14176	8.80	3.80	0.002
Cytosolic aconitase	TC15109	3.09	2.06	0.011
Ammonium assimilation				
NADH glutamate dehydrogenase	TC10856	6.97	**40.99**	0.004
Asparagine synthase	TC14104	12.16	**19.19**	0.031
Other amino acid metabolism				
Ornithine aminotransferase	TC8388	**6.31**	**7.78**	0.007
Proline dehydrogenase	TC7863	**4.51**	**10.84**	<0.001
Other metabolism				
4-Hydroxyphenylpyruvate dioxygenase (4HPPD)	TC8682	3.51	**4.93**	0.037
Cytochrome P450, isoflavone synthase	TC14262	1.76	**3.16**	0.013
Chalcone isomerase	NP591666	4.05	**4.47**	<0.001
Isoflavone reductase	TC7899	1.89	**5.52**	<0.001
Trans-cinnamate 4-monooxygenase	TC14933	1.57	**2.83**	0.046
Putative oxidoreductase	TC14685	0.81	**4.10**	0.026
NAD-dependent sorbitol dehydrogenase	TC17752	**8.46**	3.33	0.004

Gene expression in *L. japonicus* nodules harvested from plants grown under normal photoperiod (N. Ph.), or subjected to 24 h and 72 h continuous darkness, respectively. Transcript levels of these genes increased significantly (>2-fold, $P < 0.05$) under extended dark conditions and are marked in bold. The numbers indicate ratios of gene expression after 24 h and 72 h continuous darkness versus expression in the normal photoperiod (control). The *P*-value represents the level of significance between the relative gene expression levels (ANOVA).

Dark CO_2 fixation is limited under continuous darkness

The observation that the organic acid concentration and the levels of several transcripts involved in dark CO_2 fixation decreased significantly in nodules during photosynthetic carbon deficiency prompted the study of CO_2 fixation using direct $Na_2{}^{13}CO_2$ labelling of the nodulated root system. Two hours of pulse ^{13}C labelling under the normal photoperiod resulted in a substantial increase in the ^{13}C composition of nodules (Fig. 4), as expected (Fotelli *et al*., 2011). However, such an increase in ^{13}C composition of nodules was not observed in plants subjected to prolonged darkness. Nodule $\delta^{13}C$ abundance of plants subjected to 24 h and 72 h of continuous darkness was only marginally increased after 2 h of ^{13}C labelling and a 1 h chase period (Fig. 4).

Changes in total protein and amino acid content in symbiotic and non-symbiotic organs under extended dark

To test the hypothesis that increased amino acid content of nodules under photosynthetic carbon-limiting conditions was due to protein degradation, the total soluble protein content was measured in both symbiotic and non-symbiotic organs of *L. japonicus* plants subjected to prolonged darkness. Furthermore, in order to test whether the presence of nodules systemically affects the remobilization of proteins under these conditions, both 30-day-old inoculated plants harbouring nitrogen-fixing nodules and uninoculated plants, grown under the normal photoperiod or subjected to either 24 h or 72 h of extended dark, were tested. Dark treatment resulted in significantly reduced total protein levels in nodules after both 24 h and 72 h of darkness, confirming the hypothesis of protein degradation under such conditions (Fig. 5A). Reduced protein levels were also observed in stem and root of inoculated plants after 72 h of darkness. However, the total protein levels in leaves of inoculated plants remained unaltered, indicating that net protein degradation did not occur under these conditions in this organ (Fig. 5A). In contrast to inoculated plants, a reduced protein content was observed in all organs (leaves, stem, and root) of uninoculated plants after both 24 h and 72 h of extended darkness (Fig. 5B). These results indicate that nodules provided amino acids to other plant organs and thereby prevented protein degradation in leaves during darkness. To confirm this result, the amino acid concentration was quantified in leaves, stems, and roots of inoculated and uninoculated 30-day-old *L. japonicus* plants that had been subjected to extended dark periods. Amino acids accumulated in all organs under these conditions, including leaves of inoculated (Fig. 6A) and uninoculated plants (Fig. 6B) after 72 h of dark treatment. Under carbon limitation, the elevated levels of amino acids in leaves of nodulated plants, where net protein degradation did not take place, may be attributed to amino acid transfer from nodules (Fig. 7).

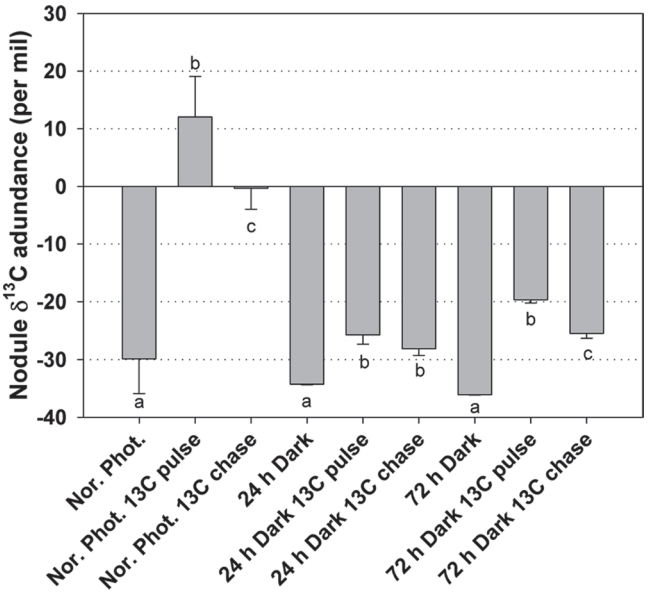

Fig. 4. $\delta^{13}C$ abundance in nodules of *L. japonicus* plants grown under a normal photoperiod, and after 24 h and 72 h of continuous dark periods, subjected to 2 h of ^{13}C pulse labelling, and 1 h of chase after the completion of the 2 h ^{13}C pulse labelling. Bars represent means (±SE) of six biological replications (three plants each). Within each light/dark condition, the statistical analysis refers to the comparison between the different labelling treatments. Significant differences ($P < 0.05$) are indicated by different letters.

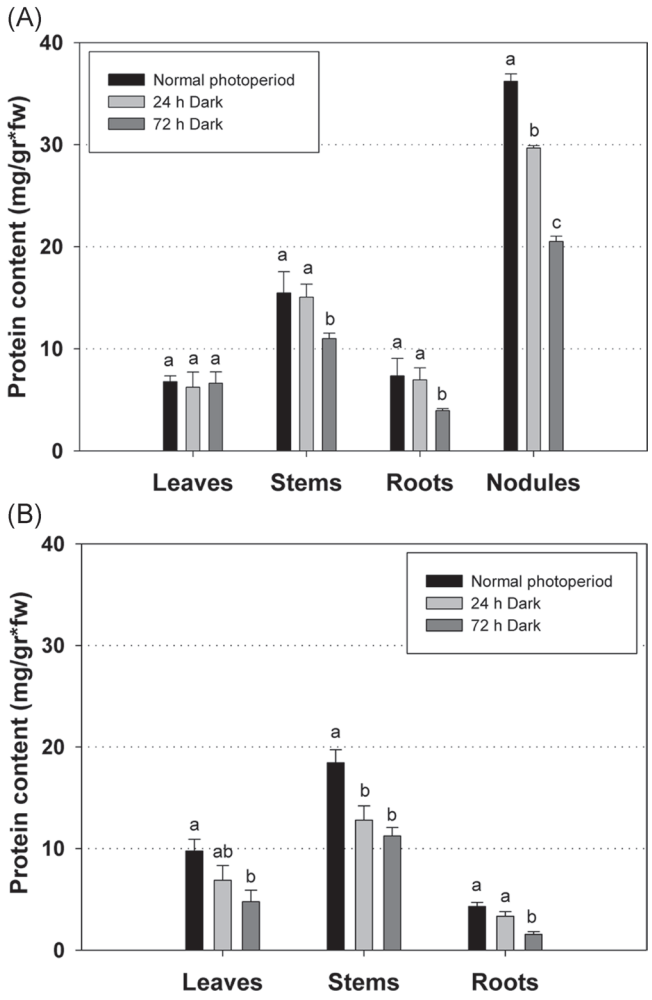

Fig. 5. Total protein content in various organs of (A) inoculated and (B) uninoculated *L. japonicus* plants during growth under a normal photoperiod and after 24 h and 72 h of continuous darkness. Bars represent means (±SE) of four biological replications. Within each graph, the statistical analysis refers to the comparison between the protein content of each organ. Significant differences ($P < 0.05$) are indicated by different letters.

Discussion

Photosynthetic carbon deficiency affects several aspects of nodule metabolism

Nodulation results in dramatic differentiation and reprogramming of multiple aspects of primary and secondary metabolism in legumes. Among the metabolic pathways upregulated during development in *L. japonicus* nodules, several were involved in C metabolism, including starch and sucrose metabolism, glycolysis, and dark CO_2 fixation (Colebatch *et al.*, 2004; Fotelli *et al.*, 2011), demonstrating the strong need for carbon and energy for nodule organogenesis and function.

In an attempt to study the effects of photosynthetic carbon deficiency on nodule metabolism, transcriptomic and metabolomic analyses were carried out in *L. japonicus* plants exposed to prolonged darkness. The length of the dark periods applied to the plants was chosen according to nodule starch content and nitrogenase activity measurements. *Lotus japonicus* exhibited a decline in nitrogenase activity of 85% after 24 h of continuous darkness (Fig. 1) but starch was still detectable in nodules, while after 72 h of darkness, nodule starch content was exhausted completely (Supplementary Fig. S1 at *JXB* online) and nitrogenase activity was decreased by 97% (Fig. 1). Although limited nitrogenase activity can be explained by different hypotheses (including interruption of photosynthesis and N feedback regulation), this dramatic decline in nitrogenase activity was attributed primarily to sugar deprivation, as it was partially restored after transferring the plants to the normal photoperiod for 48 h (Fig. 1). Consequently, even after 72 h of continuous darkness the effect of carbon starvation is still reversible.

Metabolite and transcript profiling in the present study revealed that limited photosynthate supply resulted in substantial changes, both in gene expression and in metabolite content, in nodules of dark-treated *L. japonicus* plants (Fig. 7). Interestingly, the results show that just 24 h of extended darkness was sufficient to trigger most of the variation observed in transcript levels (Fig. 3B). Changes in metabolite levels occurred more gradually during extended darkness (Fig. 2A), indicating that changes in nodule metabolism due to photosynthate limitation are mainly under transcriptional regulation, although the observed latency in metabolite changes may, in part, be accounted for post-transcriptional regulation as well.

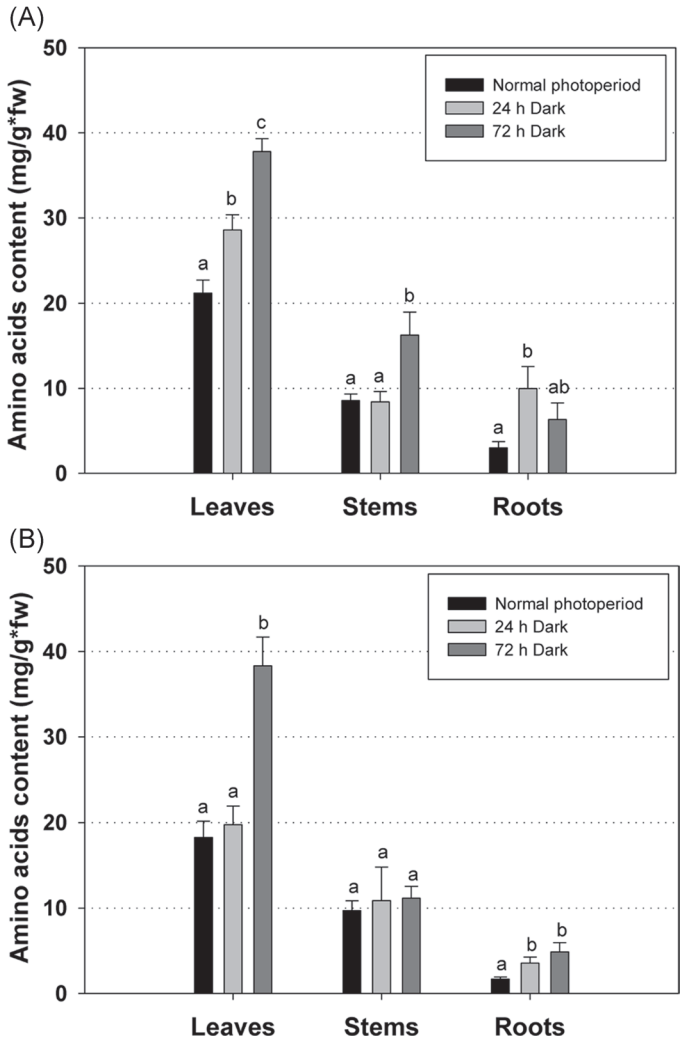

Fig. 6. Total amino acid content in leaves, stems, and roots of (A) inoculated and (B) uninoculated *L. japonicus* plants during growth under a normal photoperiod and after 24 h and 72 h of continuous darkness. Bars represent means (±SE) of four biological replications. Within each graph, the statistical analysis refers to the comparison between the total amino acid content of each organ. Significant differences ($P < 0.05$) are indicated by different letters.

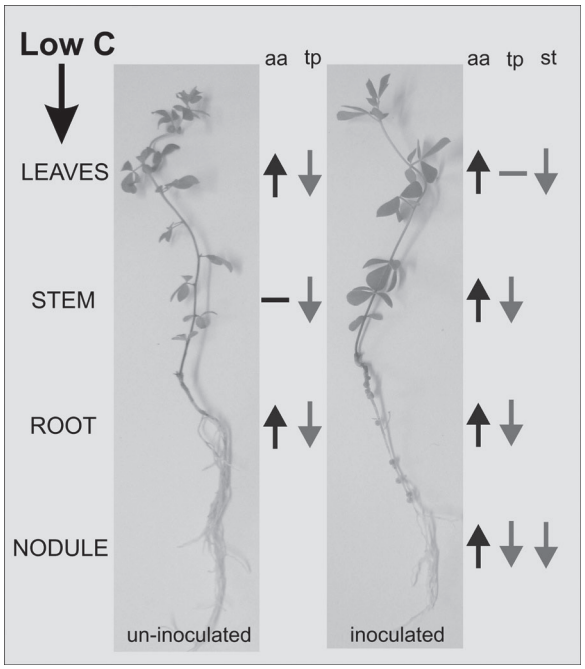

Fig. 7. Diagram of the systemic changes observed in uninfected versus infected *L. japonicus* plants under carbon-limited conditions. The high total amino acid (aa) concentration observed in all plant organs is accompanied by a reduction in total protein (tp) concentration, denoting protein degradation. In infected plants, the amino acids mobilized by protein degradation in nodules and other organs may have been a source of fixed carbon for leaves when photosynthesis was blocked, preventing protein degradation in these leaves. These results arise from the analysis of plants subjected to 72 h of continuous darkness, when starch (st) reserves were completely exhausted.

Lotus japonicus nodules showed a remarkable decline in sucrose content (Table 1), accompanied by a significant reduction of sucrose synthase transcript levels under continuous darkness (Table 2). Similarly, sucrose synthase enzymatic activity decreased to a great extent in nodules of common bean plants subjected to 2 d of darkness (Gogorcena *et al.*, 1997). Although transcript levels of several invertase genes were unaltered (Supplementary Table S2 at *JXB* online), significant induction of a gene encoding a β-fructofuranosidase (Table 3) indicates that specific members of the invertase family could play a role in the hydrolysis of sucrose under dark-stress conditions.

After 72 h of continuous darkness, the observation that the starch content was exhausted (Supplementary Fig. S1 at *JXB* online) is in accordance with the observation that three genes involved in starch synthesis (one gene coding for starch synthase and two for ADP-glucose pyrophosphorylase) were substantially down-regulated (Table 2). The other genes of starch metabolism tested did not show a significant differentiation between treatments, neither did the genes involved in starch biosynthesis nor the genes involved in starch degradation (Supplementary Table S2).

Like sucrose, the levels of a number of metabolites in the group of sugars decreased in nodules of dark-treated plants (Table 1). Glucose became undetectable after 72 h of continuous darkness, and in addition to that a down-regulation was observed in genes involved in glucose breakdown in nodules (see below).

Interestingly, during photosynthate limitation, trehalose content in nodules remained unaffected, although a plant trehalase isoform, which is likely to be involved in trehalose degradation, was found to be significantly up-regulated during prolonged darkness (Table 3). Moreover, transcripts of two plant genes coding for trehalose-6-phosphate synthase and trehalose-6-phosphate phosphatase, which are involved in trehalose synthesis, were down-regulated during extended darkness. Taken together, these results indicate that most of the measured trehalose may have been in the bacteroids. Trehalose is a well-known osmo-protectant and its biosynthesis has been linked to competitiveness of rhizobia during nodulation

(Domínguez-Ferreras *et al*., 2009). The present data indicate that trehalose, a relatively abundant disaccharide in *L. japonicus* nodules (Desbrosses *et al*., 2005), cannot be utilized as an alternative carbon source during photosynthate limitation. This result attributes different roles to trehalose in nodules, probably involving adaptation to osmotic stress.

Induction of a sorbitol dehydrogenase gene in nodules is consistent with greater polyol biosynthesis in this plant organ (Desbrosses *et al*., 2005). With the exception of mannitol, the levels of polyols were not significantly affected by photosynthate limitation. Interestingly, mannitol content was found to be >3-fold higher after 24 h of prolonged darkness. In contrast, the expression of an NADPH-dependent mannose-6-phosphate reductase, involved in mannitol biosynthesis, was found to be significantly down-regulated, whereas transcripts of mannitol and sorbitol dehydrogenase isoforms, which are involved in mannitol catabolism, were found to be significantly up-regulated. This discrepancy again may point to major participation of bacteroids in compatible solute biosynthesis and storage. Moreover, pinitol, a C-rich metabolite which is abundant in nodules (Fougère *et al*., 1991; Desbrosses *et al*., 2005), could also not be mobilized during carbon starvation in nodules, indicating that its main role is not in carbon and energy metabolism. These results suggest that polyol biosynthesis in nodules plays an alternative role, possibly in osmoregulation.

Concomitant with the depletion of sugars, a considerable number of genes involved in carbohydrate metabolism and glycolysis were found to be strongly down-regulated following dark treatment, including genes coding for phosphoglucomutase, glucose-6P isomerase, fructokinase, enolase, triosephosphate isomerase, and pyruvate decarboxylase (Table 2; Supplementary Table S2 at *JXB* online).

Sugar depletion was followed by depletion of a number of organic acids: dehydroascorbic acid, shikimic acid, ascorbic acid, succinic acid, pyruvic acid, gluconic acid, glycolic acid, D-malic acid, and oxalic acid (Table 1). The accumulation of isocitric acid (Table 1), which was found to be dark specific, can be attributed to the up-regulation of two genes coding for aconitate hydratase (Table 3).

The observation that three genes coding for both α- and β-type carbonic anhydrases and one gene coding for phosphoenolpyruvate carboxylase, which together fix CO_2 to oxaloacetate, are highly down-regulated in dark treatment (Table 2) correlates well with the observed reduction in ^{13}C incorporation in nodules under extended dark conditions (Fig. 4). Similarly, when *L. japonicus* plants were subjected to prolonged darkness and subsequent illumination, the mRNA levels and the activity of PEPC decreased and then recovered in nodules, suggesting that PEPC transcripts and activity are regulated by the amount of photosynthate transported from leaves to nodules (Nakagawa *et al*., 2003). The limited activity of this enzyme under extended darkness probably explains the high PEP accumulation observed after both 24 h and 72 h of darkness (Table 1). Limited dark CO_2 fixation also reflects on TCA accumulation, which supports N_2 assimilation in bacteroids (for a review, see Lodwig and Poole, 2003). As suspected, reduced amounts of malate were detected in the present metabolomic analysis (Table 1), coinciding with a significant decline in the expression levels of a gene coding for cytosolic malate dehydrogenase, TC7834 (Table 2). Similarly, in soybean, extended darkness was accompanied by a collapse of the malate level (Vauclare *et al*., 2010).

L-Glutamine, one of the two main amino acids assimilating ammonium, and the transcript levels of a gene encoding glutamine synthetase (TC8035) were significantly lower in nodules of dark-treated plants compared with the control (Tables 1, 2). In bean nodules, both glutamine synthetase and glutamate synthase activities decreased after plants were subjected to 1 d of darkness (Gogorcena *et al*., 1997). Moreover, the accumulation of L-alanine was substantially decreased in prolonged darkness (Table 1). Alanine is a possible alternative product of N_2 fixation in the bacteroid, under some conditions (for a review, see Day *et al*., 2001). Although ammonia is the major product of N_2 fixation when nitrogenase activity is optimized (Li *et al*., 2002), soybean bacteroids were shown to synthesize and secrete alanine under conditions of oxygen deprivation in a closed system (Waters *et al*., 1998). As in *L. japonicus*, nodules of dark-treated soybean plants showed depletion of glutamine and asparagine, and disappearance of alanine (Vauclare *et al*., 2010).

The above results are indicative of a limited carbon supply to nodules of *L. japonicus* plants under extended dark periods, resulting in dramatic nitrogenase activity reduction and limited nitrogen assimilation (Fig. 7).

Nodules can act as source organs when photosynthesis is abolished

Plants, like other organisms, have developed sophisticated mechanisms for recycling intracellular constituents under nutrient-limiting conditions. Autophagy, for example, has been suggested to play a central role in several stress responses including nutrient recycling during starvation (for a review, see Han *et al*., 2011). In the present work, photosynthetic carbon starvation resulted in significant decreases in total protein content in both symbiotic and non-symbiotic organs of *L. japonicus* plants (Fig. 5). Journet *et al*. (1986) reported that protein degradation occurs as a consequence of sucrose starvation and proposed that this protein degradation is due to autophagy. In dark-stressed bean nodules, total soluble protein decreased by 13% and 54% after 2 d and 4 d of darkness, respectively (Gogorcena *et al*., 1997). Similarly, in *Arabidopsis*, carbon starvation triggered a rapid degradation of cellular proteins and the up-regulation of autophagy-related genes (Rose *et al*., 2006). In addition, disruption of ATG (autophagy-related genes) proteins resulted in *Arabidopsis* plants that were hypersensitive to C starvation induced by extended darkness (Thompson *et al*., 2005).

Thus, the accumulation of amino acids observed in *L. japonicus* nodules after both 24 h and 72 h of extended darkness (Table 1) could be attributed to protein degradation (Fig. 5). Taylor *et al*. (2004) suggested that catabolism of branched-chain amino acids is important in providing an alternative carbon sources for oxidative phosphorylation and energy production during carbon starvation. The 40-fold increase in

transcript level for NADH-dependent glutamate dehydrogenase (GDH) (TC10856) found after 72 h of darkness (Table 3) may reflect the enzyme's role in the breakdown of amino acids to provide alternative carbon skeletons for energy production. It has been hypothesized that glutamate catabolized by GDH enters the TCA cycle as an alternative C source during C starvation (Terce-Laforgue *et al*., 2004*a*, *b*; Skopelitis *et al*., 2006). In *Arabidopsis*, NADH-dependent glutamate dehydrogenase was suggested to be a key enzyme in the breakdown of several amino acids under carbon deficiency (Miyashita and Good, 2008). Total protein declined in most organs of nodulated and non-nodulated plants following dark treatment (Fig. 5), while amino acid levels increased (Fig. 6), which indicated that protein degradation in these organs is probably the main source of the accumulating amino acids. Leaves of nodulated plants represented an exception: elevated amino acids levels (Fig. 6) were not accompanied by reduced total protein (Fig. 5). Thus, amino acids mobilized by protein degradation in nodules and other organs may have been a source of fixed carbon for leaves when photosynthesis was blocked, preventing protein degradation in these leaves (Fig. 7).

In conclusion, extended darkness was used as a tool to study the metabolic responses of nodules under photosynthetic C limitation, combining for the first time both transcript profiling and metabolomic analysis. From the data obtained, it is proposed that nodulation of the model legume *L. japonicus* results in systemic changes in the responses of the plant to photosynthate limitation triggered by the extended dark period, as nodules appeared to act as a source of both C and N, limiting protein degradation in the leaves under non-photosynthetic conditions. Although the xylem sap of *L. japonicus* could not be directly measured due to technical limitations, amino acids accumulating in nodules as a result of localized protein degradation are likely to have been transported to the shoot where they served as an alternative carbon source. Future work will aim to quantify the contribution of specific compounds exported from nodules to the total plant C budget under photosynthate limitation, using alternative legume species that allow the direct analysis of xylem sap under these conditions.

Supplementary data

Supplementary data are available at *JXB* online.

Figure S1. Starch accumulation in leaves and nodules of *L. japonicus* plants.

Figure S2. Ethylene production during the acetylene reduction assay.

Table S1. Primer pairs used in quantitative real-time PCRs.

Table S2. Gene expression in nodules after prolonged darkness.

Acknowledgements

This work was partially funded by a joint DAAD and Greek State Scholarship Foundation project and by The Samuel Roberts Noble Foundation.

References

Barsch A, Carvalho HG, Cullimore JV, Niehaus K. 2006. GC-MS based metabolite profiling implies three interdependent ways of ammonium assimilation in *Medicago truncatula* root nodules. *Journal of Biotechnology* **127,** 79–83.

Bethlenfalvay GJ, Phillips DA. 1977. Effect of light intensity on efficiency of carbon dioxide and nitrogen reduction in *Pisum sativum* L. *Plant Physiology* **60,** 868–871.

Bradford MM. 1976. Rapid and sensitive method for quantitation of microgram quantities of protein utilizing the principle of protein–dye binding. *Analytical Biochemistry* **72,** 248–254.

Colebatch G, Desbrosses G, Ott T, Krusell L, Montanari O, Kloska S, Kopka J, Udvardi MK. 2004. Global changes in transcription orchestrate metabolic differentiation during symbiotic nitrogen fixation in *Lotus japonicus*. *The Plant Journal* **39,** 487–512.

Colebatch G, Kloska S, Trevaskis B, Freund S, Altmann T, Udvardi MK. 2002. Novel aspects of symbiotic nitrogen fixation uncovered by transcript profiling with cDNA arrays. *Molecular Plant-Microbe Interactions* **15,** 411–420.

Day DA, Copeland L. 1991. Carbon metabolism and compartmentation in nitrogen-fixing legume nodules. *Plant Physiology and Biochemistry* **29,** 185–201.

Day DA, Poole PS, Tyerman SD, Rosendahl L. 2001. Ammonia and amino acid transport across symbiotic membranes in nitrogen-fixing legume nodules. *Cellular and Molecular Life Sciences* **58,** 61–71.

Desbrosses GG, Kopka J, Udvardi MK. 2005. *Lotus japonicus* metabolic profiling. Development of gas chromatography–mass spectrometry resources for the study of plant–microbe interactions. *Plant Physiology* **137,** 1302–1318.

Domínguez-Ferreras A, Soto MJ, Pérez-Arnedo R, Olivares J, Sanjuán J. 2009. Importance of trehalose biosynthesis for *Sinorhizobium meliloti* osmotolerance and nodulation of alfalfa roots. *Journal of Bacteriology* **191,** 7490–7499.

Feigenbaum S, Mengel K. 1979. The effect of reduced light intensity and sub-optimal potassium supply on N_2 fixation and N turnover in *Rhizobium*-infected lucerne. *Physiologia Plantarum* **45,** 245–249.

Flemetakis E, Efrose RC, Ott T, Stedel C, Aivalakis G, Udvardi MK, Katinakis P. 2006. Spatial and temporal organization of sucrose metabolism in *Lotus japonicus* nitrogen-fixing nodules suggests a role for the elusive alkaline/neutral invertase. *Plant Molecular Biology* **62,** 53–69.

Fotelli MN, Tsikou D, Kolliopoulou A, Aivalakis G, Katinakis P, Udvardi MK, Rennenberg H, Flemetakis E. 2011. Nodulation enhances dark CO_2 fixation and recycling in the model legume *Lotus japonicus*. *Journal of Experimental Botany* **62,** 2959–2971.

Fougère F, Le Rudulier D, Streeter JG. 1991. Effects of salt stress on amino acid, organic acid, and carbohydrate composition of roots, bacteroids, and cytosol of alfalfa (*Medicago sativa* L). *Plant Physiology* **96,** 1228–1236.

Goggin DE, Lipscombe R, Fedorova E, Millar AH, Mann A, Atkins CA, Smith PMC. 2003. Dual intracellular localization and targeting of aminoimidazole ribonucleotide synthetase in cowpea. *Plant Physiology* **131,** 1033–1041.

Gogorcena Y, Gordon AJ, Escuredo PR, Minchin FR, Witty JF, Moran JF, Becana M. 1997. N_2 fixation, carbon metabolism, and oxidative damage in nodules of dark-stressed common bean plants. *Plant Physiology* **113,** 1193–1201.

Gordon AJ, Minchin FR, James CL, Komina O. 1999. Sucrose synthase in legume nodules is essential for nitrogen fixation. *Plant Physiology* **120,** 867–878.

Gordon AJ, Ougham HJ, James CL. 1993. Changes in the levels of gene transcripts and their corresponding proteins in nodules of soybean plants subjected to dark-induced stress. *Journal of Experimental Botany* **44,** 1453–1460.

Han S, Yu B, Wang Y, Liu Y. 2011. Role of plant autophagy in stress response. *Protein and Cell* **2,** 784–791.

Handberg K, Stougaard J. 1992. *Lotus japonicus*, an autogamous, diploid legume species for classical and molecular genetics. *The Plant Journal* **2,** 487–496.

Hardy RWF, Burns RC, Holsten RD. 1973. Application of acetylene–ethylene assay for measurement of nitrogen fixation. *Soil Biology and Biochemistry* **5,** 47–81.

Hardy RWF, Havelka UD. 1976. Photosynthate as a major factor limiting nitrogen fixation by field-grown legumes with emphasis on soybeans. In: Nutman PS, ed. *Symbiotic nitrogen fixation* . Cambridge: Cambridge University Press, 421–439.

Horst I, Welham T, Kelly S, Kaneko T, Sato S, Tabata S, Parniske M, Wang TL. 2007. TILLING mutants of *Lotus japonicus* reveal that nitrogen assimilation and fixation can occur in the absence of nodule-enhanced sucrose synthase. *Plant Physiology* **144,** 806–820.

Iannetta PPM, de Lorenzo C, James EK, Fernandez-Pascual M, Sprent JI, Lucas MM, Witty JF, de Felipe MR, Minchin FR. 1993. Oxygen diffusion in lupin nodules I. Visualization of diffusion barrier operation. *Journal of Experimental Botany* **44,** 1461–1467.

Jeong J, Suh S, Guan C, Tsay YF, Moran N, Oh CJ, An CS, Demchenko KN, Pawlowski K, Lee Y. 2004. A nodule-specific dicarboxylate transporter from alder is a member of the peptide transporter family. *Plant Physiology* **134,** 969–978.

Journet E, Bligny R, Douce R. 1986. Biochemical changes during sucrose deprivation in higher plant cells. *Journal of Biological Chemistry* **261,** 3193–3199.

Kopka J, Schauer N, Krueger S, *et al.* 2005. GMD@CSB.DB: the Golm Metabolome Database. *Bioinformatics* **21,** 1635–1638.

Lawn RJ, Brun WA. 1974. Symbiotic nitrogen fixation in soybeans. I. Effect of photosynthate source–sink manipulation. *Crop Science* **14,** 11–16.

Layzell DB, Hunt S, Palmer GR. 1990. Mechanisms of nitrogenase inhibition in soybean nodules: pulse-modulated spectroscopy indicates that nitrogenase activity is limited by O_2. *Plant Physiology* **92,** 1101–1107.

Li Y, Parsons R, Day DA, Bergersen FJ. 2002. Reassessment of major products of N_2 fixation by bacteroids from soybean root nodules. *Microbiology* **148,** 1959–1966.

Liu X, Grams TEE, Matyssek R, Rennenberg H. 2005. Effects of elevated pCO_2 and/or pO_3 on C-, N-, and S-metabolites in the leaves of juvenile beech and spruce differ between trees grown in monoculture and mixed culture. *Plant Physiology and Biochemistry* **43,** 147–154.

Lodwig E, Poole P. 2003. Metabolism of *Rhizobium* bacteroids. *Critical Reviews in Plant Sciences* **22,** 37–78.

Matamoros MA, Baird LM, Escuredo PR, Dalton DA, Minchin FR, Iturbe-Ormaetxe I, Rubio MC, Moran JF, Gordon AJ, Becana M. 1999. Stress-induced legume root nodule senescence. Physiological, biochemical, and structural alterations. *Plant Physiology* **121,** 97–112.

Miyashita Y, Good AG. 2008. NAD(H)-dependent glutamate dehydrogenase is essential for the survival of *Arabidopsis thaliana* during dark-induced carbon starvation. *Journal of Experimental Botany* **59,** 667–680.

Nakagawa T, Izumi T, Banba M, Umehara Y, Kouchi H, Izui K, Hata S. 2003. Characterization and expression analysis of genes encoding phosphoenolpyruvate carboxylase and phosphoenolpyruvate carboxylase kinase of *Lotus japonicus*, a model legume. *Molecular Plant-Microbe Interactions* **16,** 281–288.

Ott T, Sullivan J, James EK, Flemetakis E, Günther C, Gibon Y, Ronson C, Udvardi M. 2009. Absence of symbiotic leghemoglobins alters bacteroid and plant cell differentiation during development of *Lotus japonicus* root nodules. *Molecular Plant-Microbe Interactions* **22,** 800–808.

Patriarca EJ, Tate R, Iaccarino M. 2002. Key role of bacterial NH_4^+ metabolism in *Rhizobium*–plant symbiosis. *Microbiology and Molecular Biology Reviews* **66,** 203–222.

Ramakers C, Ruijter JM, Deprez RH, Moorman AF. 2003. Assumption-free analysis of quantitative real-time polymerase chain reaction (PCR) data. *Neuroscience Letters* **339,** 62–66.

Rose TL, Bonneau L, Der C, Marty-Mazars D, Marty F. 2006. Starvation-induced expression of autophagy-related genes in Arabidopsis. *Biology of the Cell* **98,** 53–67.

Sarath G, Pfeiffer NE, Sodhi CS, Wagner FW. 1986. Bacteroids are stable during dark-induced senescence of soybean root nodules. *Plant Physiology* **82,** 346–350.

Schauer N, Steinhauser D, Strelkov S, *et al.* 2005. GC-MS libraries for the rapid identification of metabolites in complex biological samples. *FEBS Letters* **579,** 1332–1337.

Skopelitis DS, Paranychianakis NV, Paschalidis KA, *et al.* 2006. Abiotic stress generates ROS that signal expression of anionic glutamate dehydrogenases to form glutamate for proline synthesis in tobacco and grapevine. *The Plant Cell* **18,** 2767–2781.

Streeter JG. 1995. Recent developments in carbon transport and metabolism in symbiotic systems. *Symbiosis* **19,** 175–196.

Swaraj K, Laura JS, Bishnoi NR. 1994. Dark treatment effects on nitrogen fixation and enzymes associated with scavenging hydrogen peroxide in clusterbean nodules. *Plant Physiology and Biochemistry* **32,** 115–119.

Taylor NL, Heazlewood JL, Day DA, Miller AH. 2004. Lipoic acid-dependent oxidative catabolism of α-keto acids in mitochondria provides evidence for branched-chain amino acid catabolism in Arabidopsis. *Plant Physiology* **134,** 838–848.

Temple SJ, Vance CP, Gantt JS. 1998. Glutamate synthase and nitrogen assimilation. *Trends in Plant Science* **3,** 51–56.

Tercé-Laforgue T, Dubois F, Ferrario-Méry S, Pou de Crecenzo MA, Sangwan R, Hirel B. 2004*a*. Glutamate dehydrogenase of

tobacco is mainly induced in the cytosol of phloem companion cells when ammonia is provided either externally or released during photorespiration. *Plant Physiology* **136,** 4308–4317.

Tercé-Laforgue T, Mäck G, Hirel B. 2004*b*. New insights towards the function of glutamate dehydrogenase revealed during source–sink transition of tobacco (*Nicotiana tabacum*) plants grown under different nitrogen regimes. *Physiologia Plantarum* **120,** 220–228.

Thompson AR, Doelling JH, Suttangkakul A, Vierstra RD. 2005. Autophagic nutrient recycling in Arabidopsis directed by the ATG8 and ATG12 conjugation pathways. *Plant Physiology* **138,** 2097–2110.

Tricot F. 1993. Mise en place des nodosites du pois proteagineux de printemps (*Pisum sativum* L.). Influence de la nutrition carbonee. PhD thesis, Universite Paris-Sud Orsay.

Udvardi MK, Day DA. 1997. Metabolite transport across symbiotic membranes of legume nodules. *Annual Review of Plant Physiology* **48,** 493–523.

Udvardi MK, Price GD, Gresshoff PM, Day DA. 1988. A dicarboxylate transporter on the peribacteroid membrane of soybean nodules. *FEBS Letters* **231,** 36–40.

Vauclare P, Bligny R, Gout E, De Meuron V, Widmer F. 2010. Metabolic and structural rearrangement during dark-induced autophagy in soybean (*Glycine max* L.) nodules: an electron microscopy and ^{31}P and ^{13}C nuclear magnetic resonance study. *Planta* **231,** 1495–1504.

Waters JK, Hughes BL 2nd, Purcell LC, Gerhardt KO, Mawhinney TP, Emerich DW. 1998. Alanine, not ammonia, is excreted from N_2-fixing soybean nodule bacteroids. *Proceedings of the National Academy of Sciences, USA* **95,** 12038–12042.

White J, Prell J, James EK, Poole P. 2007. Nutrient sharing between symbionts. *Plant Physiology* **144,** 604–614.

Winter H, Lohaus G, Heldt W. 1992. Phloem transport of amino acids in relation to their cytosolic levels in barley leaves. *Plant Physiology* **99,** 996–1004.